RJC

RASĀYAN ***J. Chem.***
Vol. 18 | No. 4 |1993-1998| October-December | 2025
ISSN: 0974-1496 | e-ISSN: 0976-0083 | CODEN: RJCABP
http://www.rasayanjournal.com
http://www.rasayanjournal.co.in

ENVIRONMENTALLY SYNTHESISED YELLOW FLUORESCENT CARBON DOTS FOR ANTIBACTERIAL APPLICATIONS

Aniza Salviana Prayugo[1], Marpongahtun[2,✉], Saharman Gea[2] and Heri Sutanto[3]

[1]Postgraduate Program of Chemistry, Faculty of Mathematics and Natural Science, Universitas Sumatera Utara, Medan, 20155, Indonesia
[2]Department of Chemistry, Faculty of Mathematics and Natural Science, Universitas Sumatera Utara, Medan, 20155, Indonesia
[3]Department of Physics, Faculty of Science and Mathematics, Universitas Diponegoro, Jawa Tengah, 50275, Indonesia
✉Corresponding author: marpongahtun@usu.ac.id

ABSTRACT

Carbon dots (CDs) are carbon-based zero-dimensional and show potential in antimicrobial infections. In this study, CDs were synthesized from p-aminophenol and ethylenediamine using the hydrothermal process at 180°C for 12 h. The UV-Vis absorption spectrum exhibits a peak at 240 nm, indicating the π-π* shift of sp^2 carbon, with an energy gap of 3.3 eV. Yellow fluorescence was observed in the CDs, with dual emission at 509 nm and 544 nm. The PL QY of CDs was about 44%. CDs appear spherical in HR-TEM images, with an average size of 4.2 nm, and are aggregated due to high surface energy. FTIR spectra show an adsorption peak at 1479.34 cm^{-1}, indicating C=C stretching. XRD shows the broad peaks around 25.5° linked to (002) lattice planes of amorphous carbon. CDs have been shown to kill any bacteria, with the maximum zone of inhibition at 10 wt% CDs.

Keywords: Carbon Dots, P-Aminophenol, Ethylenediamine, Hydrothermal, Antibacterial Activity.

RASĀYAN *J. Chem.*, Vol. 18, No.4, 2025

INTRODUCTION

Carbon dots (CDs) are fluorescent carbon-based nanomaterials (<10 nm) that have gained popularity among researchers since 2004, due to their distinct optical characteristics, low toxicity, biocompatibility, simple synthetic routes, and low cost.[1] Carbon dots are manufactured and used in various applications, including optoelectronic devices[2], biological labeling[3], biomedicine[4], photocatalysis[5], and antibacterial.[6] The accessible surface states, adaptable photoexcited states, and photo-electron transfer properties keep the sterilisation of CDs viable and are progressively gaining acceptance in the antibacterial field.[7] Since their discovery in 2004, CDs have emerged as a potential alternative to conventional antibiotics. Several antimicrobial actions of CDs have been verified in many studies. The antimicrobial mechanism of CDs involves their small size and high surface area, facilitating attachment to the bacterial surface and entry into the cell. The specific antimicrobial process involves CDs attaching to the external cell surface, blocking nutrient uptake by bacteria. Furthermore, through electrostatic interactions, CDs cause damage to the cell membrane, leading to leakage of cell contents. Finally, CDs enter the cell and disrupt DNA, RNA, and protein structures through noncovalent bonding.[8] P-aminophenol is a biocompatible aromatic organic compound, primarily used to manufacture paracetamol. This compound can inhibit the growth of bacteria, fungi, and other organisms. This eliminates the disadvantage of typical precursor CDs, which are unable to address bacterial polymeric compounds.[9] The weakness of CDs synthesized from chemical compounds is the relatively low fluorescence intensity with a quantum yield (QY) <10%.[10] Ethylenediamine, a nitrogen source, overcomes this by enhancing electron mobility, generating more charge carriers. Therefore, modifying the CDs surface can improve its quantum yield.[11] For instance, Zhang *et al.* prepared yellow emission CDs by adding fullerene carbon soot, dissolved in HNO_3 and H_2SO_4 (QY 3-5%).[12] However, the solvents used in this type of synthesis route are highly toxic, corrosive, and unfriendly to the environment.

http://doi.org/10.31788/RJC.2025.1849427

Thus, it limits biocompatibility in antibacterial activity.[13] Similarly, Nawas et al. acquired yellow emission CDs with citric acid, urea, and polyethyleneimine as carbon sources with DMF as solvent via the hydrothermal technique (160 °C, 5h).[14] DMF may not be the ideal solvent because it interferes with the emission or aggregation of the CDs.[15] Kavitha and his team used biochar as raw materials to acquire yellow-CDs.[16] The drawback of CDs from biomass is their poor stability. Meanwhile, Nitrogen atoms can generate stable carbon nuclei and enhance core stability, reducing aggregation and low toxicity when combined with other CDs synthesis precursors.[17] In this study, we synthesised yellow CDs using a hydrothermal technique by integrating p-aminophenol and ethylenediamine to improve their efficacy for antibacterial applications.

EXPERIMENTAL

Materials

Ethylenediamine, p-aminophenol, and deionized water were bought from Merck. Nutrient Agar was purchased from Merck, and *Staphylococcus aureus* (*S. aureus*) (ATCC 25923) and *Escherichia coli* (*E. coli*) (ATCC 25922) from Sigma-Aldrich. All of the materials were used, requiring no further purification.

Synthesis of CDs

CDs were synthesised via the hydrothermal technique. Initially, 0.2 g of p-Aminophenol was combined with 11 mL of deionized water and 4 mL of ethanol. After 15 min of stirring this solution, 0.125 mL of ethylenediamine was added dropwise. The solution was heated to 180°C for 12 h in a 100 mL autoclave lined with Teflon. A 15-min centrifugation at 11,000 rpm was performed on the solution following the reaction. Following centrifugation, the solution was processed using a 0.22 μm Millipore membrane syringe filter, yielding the CDs solution.

Antibacterial Test

The antibacterial activity was assessed using the agar disk diffusion technique. Both *E. coli* and *S. aureus* pure strains were uniformly inoculated onto Nutritional Agar plates. Paper disks, 6 mm in diameter, sterile, were soaked in CDs and then carefully placed on the agar surface. The diameter of the inhibitory zones on the plates was measured in millimetres following a 24-hour incubation period at 36°C.

Measurement of Quantum Yield

To investigate the quantum yield (QY) of CDs, utilise the equation (1) with quinine sulphate solution in 0.1 M H_2SO_4 (QY = 54% and η = 1.33) at 360 nm reference.[12]

$$\mathrm{QYc} = QYs \times \frac{Ic}{Is} \times \frac{As}{Ac} \times \left(\frac{\eta c}{\eta s}\right)^2 \quad (1)$$

The quantity of yield (QY) matches the emission fluorescence brightness. A is the absorbance, I measured under the excitation wavelength, and η is the solvent refractive index. C and S for CDs, and quinine sulphate. Photoluminescence spectrum from Fluorescence Spectrometer.

Detection Method

HRTEM images were taken with a JEOL-2100 TEM. A PerkinElmer spectrometer was used to record Fourier-transform infrared spectroscopy (FTIR) spectra. Optical absorption spectra were measured using a Shimadzu UV-1800 spectrophotometer. Photoluminescence (PL) spectra were obtained with a PerkinElmer LS45 fluorescence spectrometer. A Rigaku MiniFlex II was used to analyze solid-state CDs via X-ray Diffraction (XRD). Antibacterial investigations on Gram-negative and Gram-positive bacteria were conducted in the biological laboratory at Universitas Sumatera Utara.

RESULTS AND DISCUSSION

The Optical Properties of CDs

CDs formed a brown liquid in sunlight and luminesced yellow-green under UV lamp, as seen in the inset Fig.-1a. Two-emission behaviour was caused by CDs fluorophores with different energy levels. The UV-Vis spectrum (Fig.-1a) has absorbance at 240 nm and 378 nm, respectively. Linked C=C bond π-π* electron transition in sp^2 aromatic carbon core and n-π* shift in surface group function (C=O, C-N) are related.[18]

The bandgap values of the CDs are illustrated in Fig.-1c, derived by the Tauc-plot approach. The energy band measures 3.3 eV, and maintains the energy bandgap values of CDs in the 1.5–3.5 eV range found in earlier research,[19] Indicates the CDs capability for photocatalytic activation under visible light, generating reactive oxygen species harmful to bacterial cells. [20]

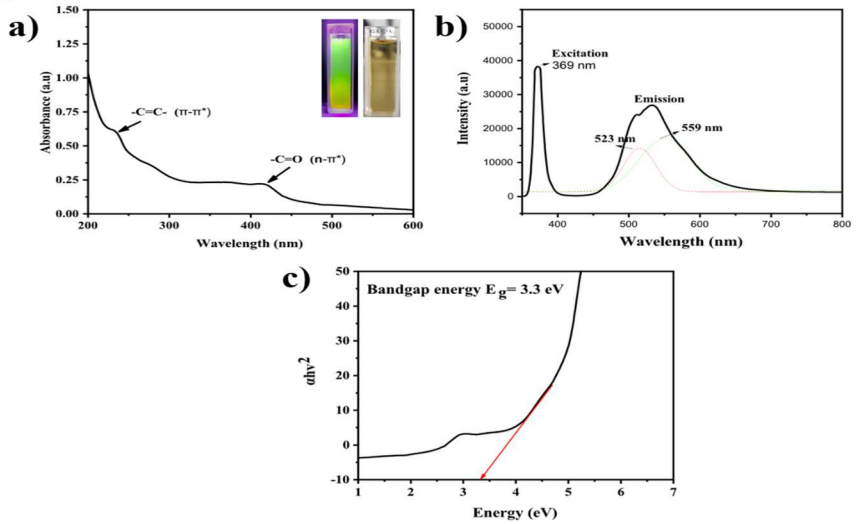

Fig.-1: (a) UV-Vis Absorption Spectrum, (b) Fluorescence Photoluminescence Spectra, and (c) Band Gap of CDs

The fluorescence emission spectrum of CDs in aqueous solution was measured using photoluminescence spectrophotometry as shown in Fig.-1b. The CDs produced dual emission peaks at 509 nm and 544 nm, with an excitation peak at 369 nm (Gaussian-adjusted).[21] The green emission of the short wavelength is from carbon core states through radiative recombination between electrons trapped on the surface and holes. Whereas the yellow emission for the length wavelength is from the surface states (C=O and COOH).[22] The difference in emission color is determined by the location of the electron-hole recombination within the CDs structure. A quantum yield (QY) of 44% for CDs, determined using quinine sulfate as a reference, indicates high fluorescence intensity retention, demonstrating both solubility and biocompatibility.

Particle Morphology and Structure of CDs

The morphological and size distribution of the CDs were assessed using HR-TEM, as illustrated in Fig.-2 (a and b). CDs exhibit a spherical or dot-like shape, are small, monodisperse, and aggregated due to the high surface energy. An average size of 4.2 nm, with a particle size range of 1–9 nm. These nonspherical CDs can influence their interaction and aggregation.[23] The carbon chains continuously grow into the core through a sustained polymerization process, and sizes below 10 nm have cellular uptake capabilities, thereby avoiding potential toxicity.[24]

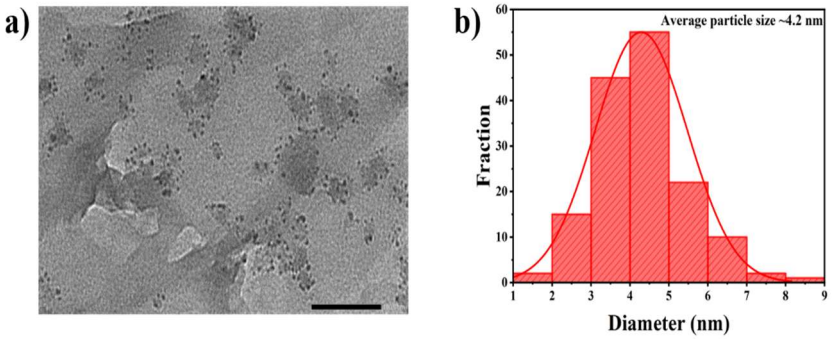

Fig.-2: Morphology of (a) TEM images of CDs and (b) Size Distribution of CDs

FTIR and XRD were used to determine the chemical composition and surface characteristics of CDs. The XRD characterization was performed to further investigate the CDs, the structure can be seen in Fig.-

3a. A broad diffraction peak at 25.5° relates to the diffraction peak (002), showing the amorphous carbon resulting from the deformation of sp^3 carbon defects in the graphite lattice. This suggests that CDs have a specific crystalline structure alongside amorphous areas.[25] The functional group structure was analysed using FTIR (Fig.-3b). The FTIR showed that CDs have N–H and O–H stretching bands at 3434.51 cm^{-1}. The C=C vibration is responsible for the strong 1479.34 cm^{-1} and 1382.48 cm^{-1} peaks are due to waves of C–N stretching. The aromatic ring C–H stretching is indicated by the peak at 2923.01 cm^{-1}, while the peaks at 1665.14 cm^{-1} and 1234.03 cm^{-1} relate to the vibrations of the carbonyl C=O and ether C–O groups.[26] A variety of oxygenated functional groups certainly contribute to their water solubility.

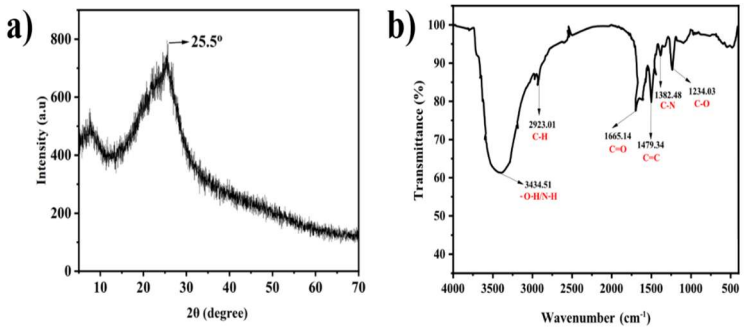

Fig.-3: (a) XRD and (b) FTIR Spectrum of CDs

Antibacterial Activity

CDs were investigated as antibacterial agents against Gram-negative and Gram-positive bacteria, including *E. coli* and *S. aureus*. Streptomycin was employed as a control for the antimicrobial investigation, and the well size was 6 mm. We used the well-established and straightforward agar-diffusion disk method for antibacterial strains. The antimicrobial effect of CDs improves with increasing concentration, as seen in Fig.-4. CDs had a mass fraction of 10 wt%, demonstrating their ability to inhibit *E. coli* and *S. aureus* with zone diameters of 8.1 mm and 3.3 mm, respectively, which is seen in Fig.-5. This was mainly due to CDs destroying the bacterial structure of *E. coli* and *S. aureus*, as well as causing irreversible cell damage via oxidative stress. The pore size of CDs, both in their basal and stimulated states, can inhibit the formation of reactive oxygen species (ROS), limiting their capacity to kill bacteria in certain applications.[27] Some studies have also concluded that CDs with added ethylenediamine or nitrogen heteroatoms exhibit better antibacterial activities than CDs generated from biomass.[28]

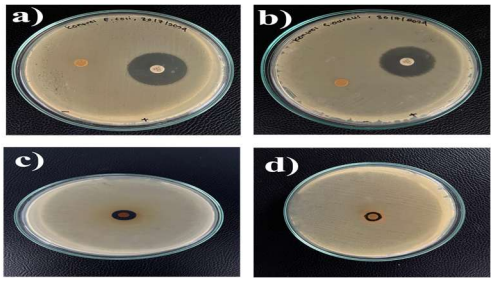

Fig.-4: Agar Well Diffusion Method at 1 wt.% CDs and Control of (a) *E. coli*, (b) *S. aureus,* (c), and (d) at 10 wt.% CDs

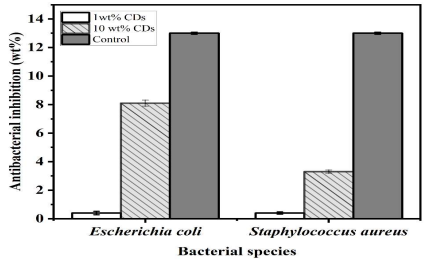

Fig.-5: CDs Concentrations and Inhibition Zone Dimensions Antimicrobial Activity

CONCLUSION

Hydrothermal synthesis of water-soluble fluorescent carbon dots was done. UV-Vis analysis revealed a π-π* transition at 240 nm, with an energy gap of 3.3 eV. Yellow fluorescence was shown at 544 nm and 509 nm, with dual emission peaks. About 44% PL QY. HRTEM shows CDs at 4.2 nm. FTIR shows C=C (1479.34 cm^{-1}) stretching. The XRD diffractogram shows amorphous carbon. Bacterial growth inhibition containing CDs decreased rapidly as the CDs concentration. It means that as the concentration increases, CDs have a better chance of bonding to bacterial cell walls and affecting them. It can effectively inhibit bacterial growth. The lowest concentration of bacterial agents that shows an identity for *E. coli* and *S. aureus* is 10 wt% CDs.

ACKNOWLEDGMENTS

The author acknowledges the Ministry of Education, Culture, Research, and Technology of Indonesia for funding the 2024 PDD Research Grant No: 69/UN5.4.10. S/PPM/KP-DRTPM/2024.

CONFLICT OF INTERESTS

There are no conflicts of interest to declare.

AUTHOR CONTRIBUTIONS

The present work is related to *SDG-3: Good Health and Well-being*. All the authors contributed significantly to this manuscript, participated in reviewing/editing and approved the final draft for publication. The research profile of the authors can be verified from their ORCID ids, given below:

A. Salviana Prayugo https://orcid.org/0009-0003-9567-2554
Marpongahtun https://orcid.org/0000-0003-1050-0431
S. Gea https://orcid.org/0000-0003-0615-0918
H. Sutanto https://orcid.org/0000-0001-7119-9633

REFERENCES

1. J. Liu, R. Li, and B. Yang, *ACS Central Science,* **6**, 2195(2020), https://dx.doi.org/10.1021/acscentsci.0c01306
2. A. S. Prayugo, Marpongahtun, S. Gea, A. Daulay, M. Harahap, J. Siow, R. Goei, A.I.Y. Tok, *Biosensors and Bioelectronics: X*, **14**, 100363(2023), https://doi.org/10.1016/j.biosx.2023.100363
3. S. Sattariazar, S. N. E. Himi, N. Arsalani, and F. Kazeminava, *Colloids and Surfaces B: Biointerfaces*, **232**, 113603(2023), https://doi.org/10.1016/j.colsurfb.2023.113603
4. M. Jiao, Y. Wang, W. Wang, X. Zhou, J. Xu, Y. Xing, L. Chen, Y. Zhang, M. Chen, K. Xu, S. Zheng, *The Chemical Engineering Journal*, **440**, 135965(2022), https://doi.org/10.1016/j.cej.2022.135965
5. Marpongahtun, Andriayani, Y. Muis, S. Gea, S. A. Amaturrahim, B. Attaurazaaq, A. Daulay, Salmiati, *Chemistry Africa*, **7**, 3328(2024), https://doi.org/10.1007/s42250-024-00970-x
6. Ezati P, Rhim JW, Molaei R, Priyadarshi R, Roy S, Min S, *Sustainable Material Technology*, **32**, 2021, https://doi.org/10.1016/j.susmat.2022.e00397
7. W. B. Zhao, K. K. Liu, Y. Wang, F. K. Li, R. Guo, S.Y Song, C. X. Shan, *Advanced Healthcare Materials*, **12**, 2300324(2023), https://doi.org/10.1002/adhm.202300324
8. F. Lin, Z. Wang, and F. G. Wu, *Pharmaceuticals (Basel),* **15**, 1236(2022), https://doi.org/10.3390/ph15101236
9. B. Pant, P. Pokharel, A. P. Tiwari, P. S. Saud, M. Park, Z.K. Ghouri, S. Choi, S.J. Park, H Y. Kim, *Ceramics International*, **41**, 5662(2015), https://doi.org/10.1016/j.ceramint.2014.12.150
10. T. Balakrishnan, W.L. Ang, E. Mahmoudi, A.W. Mohammad, and N.S. Sambudi, *Carbon Resources Conversion*, **5**, 166(2022), https://doi.org/10.1016/j.crcon.2022.01.003
11. A. Daulay, L.H. Nasution, M. Huda, M. Amin, M. Nikmatullah, *Biosensors and Bioelectronics: X*, **17**, 100460(2024), https://doi.org/10.1016/j.biosx.2024.100460

12. Q. Zhang, X. Sun, H. Ruan, K. Yin, and H. Li, *Science China Materials,* **60**, 150(2017), https://doi.org/10.1007/s40843-016-5160-9
13. P. Li, L. Sun, S. Xue, D. Qu, L. An, X. Wang, Z. Sun, *SmartMat*., **3,** 248(2022), https://doi.org/10.1002/smm2.1131
14. Z.N. Sherif and K. Anitha, *Materials Research Bulletin*, **190**, 113509(2025), https://doi.org/10.1016/j.materresbull.2025.113509
15. H. Yang, Y. Liu, Z. Guo, B. Lei, J. Zhuang, X. Zhang, Z. Liu, C. Hu, *Nature Communications*, **10**, 1789(2019), https://doi.org/10.1038/s41467-019-09830-6
16. X. Liao, X. Lu, H. Zou, X. Hu, Y. Xiong, J Cao, J. Pan, C. Li, Y. Zheng, *Materials Today Communications*, **35**, 106383(2023), https://doi.org/10.1016/j.mtcomm.2023.106383
17. C. Zhao, X. Li, C. Cheng, and Y. Yang, *Microchemical Journal* **147**, 190 (2019), https://doi.org/10.1016/j.microc.2019.03.029
18. X. Liu, Y. Zhang, S. Gao, H. Xing, D. Wang, H. Hu, X. Qian, D. Chen, *Analytica Chimica Acta*, **1367**, 344319(2025), https://doi.org/10.1016/j.aca.2025.344319
19. H. Sutanto, I. Alkian, N. Romanda, I.W.L. Lewa, I. Marhaendrajaya, and P. Triadyaksa, *AIP Advances,* **10**, 04595(2020), https://doi.org/10.1063/5.0004595
20. M. Karbasi, F. Karimzadeh, K. Raeissi, S. Ritmi, J. Kiwi, S. Giannakis, C. Pulgarin, *Water*, **12**, 1099(2020), https://doi.org/10.3390/w12041099
21. O. Dimitriev, D. Kysil, A. Zaderko, O. Isaieva, A. Vasin, Y. Pirayatinski, M. Fahlman, A. Nazarov, *Nanoscale Advances*, **6**, 2197(2024), https://doi.org/10.1039/d4na00033a
22. P. Zhang, Y. Zheng, L. Ren, S. Li, M. Feng, Q. Zhang, R. Qi, Z. Qin, J. Zhang, L. Jiang, *Nanomaterials*, **14**, 970(2024), https://doi.org/10.3390/nano14110970
23. Y. Ru, G. I. N. Waterhouse, and S. Lu, *Aggregate*, **3**, 296(2022), https://doi.org/10.1002/agt2.296
24. J. Dolai, K. Mandal, and N.R. Jana, *ACS Applied Nano Materials,* **4**, 987(2021), https://doi.org/10.1021/acsanm.1c00987
25. D. Cai, X. Zhong, L. Xu, Y. Xiong, W. Deng, H. Hou, X. Ji., *Chemical Science*, **16**, 4970(2025), https://doi.org/10.1039/d4sc08659g
26. R.B.G. González, L.T.González, M. Madou, C. L. Porras, S.O.M. Chapa, and A. Mendoza, *Nanomaterials*, **12**, 3390(2022), https://doi.org/10.3390/nano12030298
27. L. Quan, W. Jiang, H. Li, H. Li, Q. Wang, and L. Chen, *Biosystems Engineering*, **216**, 1016(2022), https://doi.org/10.1016/j.biosystemseng.2022.01.019
28. F. Wen, P. Li, H. Meng, H. Yan, X. Huang, H. Cui, W. Su, *et al.*, *Photodiagnosis and Photodynamic Therapy,* **39**, 103033(2022), https://doi.org/10.1016/j.pdpdt.2022.103033

[RJC-9427/2025]